JOURNAL OF THE MECHANICAL BEHAVIOR OF BIOMEDICAL MATERIALS ▮ (▮▮▮▮) ▮▮▮–▮▮▮

Available online at www.sciencedirect.com

ScienceDirect

www.elsevier.com/locate/jmbbm

Transient behavior and relaxation of microcapsules with a cross-linked human serum albumin membrane

*Pierre-Yves Gires, Dominique Barthès-Biesel, Eric Leclerc, Anne-Virginie Salsac**

Biomechanics and Bioengineering Laboratory (UMR CNRS 7338), Université de technologie de Compiègne - CNRS, Sorbonne université, CS 60319, 60203 Compiègne, France

ARTICLE INFO

Article history:
Received 7 June 2015
Received in revised form
6 September 2015
Accepted 8 September 2015

Keywords:
Microcapsules
Relaxation
Microfluidic experiment
Mechanical characterization
Fluid structure interactions

ABSTRACT

Capsules consist of droplets enclosed by a membrane with shear resistant properties especially when fabricated by interfacial cross-linking. In many applications, the protection and release of the internal medium need to be strictly controlled. It is possible to tune the membrane mechanical properties by changing the physico-chemical conditions of the fabrication process, but a good control of the production requires their characterization, which is a scientific challenge, since the objects are a few tens of microns in size at most. One advantageous approach is to resort to microfluidic techniques. We study the transient response of capsules having a cross-linked human serum albumin (HSA) membrane, as they flow through a sudden expansion. We determine the characteristic time scales of the capsule relaxation and compare them to the ones predicted by a full numerical model of the relaxation of a capsule flowing in a rectangular channel, for which the membrane is assumed to be purely elastic. We show that the membrane is viscoelastic and that the relaxation is solely a function of the ratio of the relaxation time to the convective time.

1. Introduction

Capsules, which are liquid droplets enclosed by a thin elastic membrane, are widely found in nature (red blood cells, fish eggs). Among all their industrial and clinical applications, one can highlight their extensive use in cosmetics and the great potential they offer in bioengineering and in medicine: by encapsulating drugs, genetic material or cells, capsules have found applications in targeted drug delivery and in the development of bioartificial organs and biosensors (Orive et al., 2004; Lam and Gambari, 2014). The deformable membrane that separates the internal and external liquids controls the potential diffusion and degradation of the internal substance, as well as its rate of release when it occurs.

Artificial capsules can be obtained through gelation or interfacial polymerization of a liquid droplet. The current fabrication processes tend to lead to approximately spherical particles enclosed by a thin membrane with mechanical properties that depend on the fabrication procedure. The membranes can be made of natural constituents such as alginate, poly-L-lysine and proteins (Kühtreiber et al., 1999; Edwards-Lévy, 2011), or of synthetic polymers such as polyamid and polysiloxane (Walter et al., 2000; Koleva and Rehage, 2012). Poly-L-lysine and alginate membranes rely on electrostatic interactions between negatively and

*Corresponding author.
E-mail address: a.salsac@utc.fr (A.-V. Salsac).

http://dx.doi.org/10.1016/j.jmbbm.2015.09.008
1751-6161/

positively charged ions and consist of a gel. Protein and synthetic polymeric membranes are in contrast produced through interfacial cross-linking, which generates covalent bonds across molecules. The resulting membranes thus differ in mechanical properties. Cross-linked membranes have been shown to be more resistant to external constraints (Kühtreiber et al., 1999).

The motion and deformation of flowing capsules depend on the mechanical properties of the membrane. The behavior of artificial spherical capsules with a cross-linked membrane has been observed under steady simple shear flow (Walter et al., 2000; Koleva and Rehage, 2012; Chang and Olbricht, 1993; Rehage et al., 2002) and planar hyperbolic flow (Chang and Olbricht, 1993; Barthès-Biesel, 1991; de Loubens et al., 2014). Experimental studies show that the capsule takes in both cases an approximately ellipsoidal shape, which depends on the ratio between the flow strength and the membrane elastic resistance to deformation. The difference is that, in simple shear flow, the flow vorticity leads to membrane rotation around the steady capsule deformed shape.

The influence of confinement has been studied more recently by flowing millimetric or micrometric size capsules through cylindrical tubes (Risso et al., 2006; Lefebvre et al., 2008; Chu et al., 2011) or through square section microfluidic pores (Leclerc et al., 2012; Hu et al., 2013). In all the cases, the particle is deformed by the flow and reaches a steady-state shape, for which the membrane (and thus the inner fluid) is immobile within the reference frame of the flowing capsule. The capsule then takes the form of a slug or has a parachute shape at the rear depending on the confinement, flow strength and capsule rigidity.

One practical application of experiments of flowing capsules is to measure the mechanical properties of the membrane. Their identification requires comparing the experimental steady-state results with a suitable fluid–structure interaction model that simulates the same conditions as those prevailing in the experiment. The shear flow experiments can be analyzed with the asymptotic model of Barthès-Biesel and Rallison (1981), when the deformation is small to moderate. The pore flow experiments are analyzed by means of a full numerical model of the set–up, where the capsule membrane is assumed to have purely hyperelastic properties (Lefebvre et al., 2008; Hu et al., 2012). Since the membrane is motionless at equilibrium, the model is also appropriate to represent the equilibrium deformation of a capsule with a viscoelastic membrane. It has been shown that such models allow to correlate the membrane mechanical properties of cross-linked ovalbumin membranes to the physicochemical conditions of the capsule fabrication and thus to the cross-linking degree (Chu et al., 2011).

Thanks to the rapidly growing microfluidic technologies it is possible to design devices that are more complex than a straight uniform pore. Owing to fabrication constraints, the tubes usually have a square or rectangular cross-section. The objective of the paper is to investigate the feasibility of using a microfluidic channel with a sudden expansion to study the relaxation of a population of capsules subjected to varying flow conditions in order to detect whether there is any membrane viscosity. Very few experimental studies have investigated the membrane viscosity of artificial capsules. Chang and Olbricht (1993) considered 2 to 4-mm size capsules with nylon membranes and followed their transient shape and orientation under Couette flow. They obtained an estimate of the membrane viscosity and elastic Young modulus from a comparison of the experimental deformation to the one predicted by the small-deformation theoretical model of Barthès-Biesel and Sgaier (1985). A larger number of experimental techniques have, however, been developed in the 1970s and 1980s to determine the membrane viscosity of red blood cells. They involve quite complex experimental setups based on the time-dependent recovery after the removal of micropipette aspiration (Chien et al., 1978) or of an elongating traction force (Hochmuth et al., 1979), or else on the measurement of the tank-treading frequency (Tran-Son-Tay et al., 1984). Recently, Tomaiuolo et al. (2011) have measured the transient deformation of red blood cells flowing in a microfluidic diverging channel. Using a Kelvin–Voigt model for the global deformation of the cells, they obtained an estimate of the membrane viscosity.

In the present study, the transient behavior of artificial capsules with a diameter of the order of 120 μm will be investigated in a microfluidic channel composed of a square section tube followed by a co-axial rectangular one. The experimental results will be compared to a numerical simulation of the relaxation of a capsule from a square channel to a rectangular one in the case of a purely hyperelastic capsule membrane. The capsule will be released into the rectangular channel with the deformed shape that it takes at steady state in the square channel. By comparing the characteristic times of relaxation obtained in the numerical and experimental cases, we will be able to determine whether the capsule membrane is viscoelastic or purely elastic.

2. Materials and methods

2.1. *Preparation of capsules suspensions*

Capsules are prepared from an emulsion of droplets of aqueous buffered human serum albumin (HSA) solutions (pH 8) suspended in cyclohexane, in which are added a surfactant (sorbitan trioleate) and the cross-linking agent (terephthaloyl chloride). Two mass concentrations of HSA are considered: [HSA]=20% and 30% (weight/volume), which correspond to 20 or 30 g of solute dissolved in 100 mL of the aqueous solution (these concentration units are the ones that are classically used in chemistry and biology). In the following, the two capsule populations will be denoted HSA20 and HSA30. The reaction time is 30 min and the stirring speed is 1700 rpm. The diameters of the investigated capsules lie in the range 110–124 μm, with an average value of 119 μm. After fabrication, the capsules are rinsed successively in an aqueous solution of polysorbate, and thrice in pure water. They are then transferred into glycerol for storage.

2.2. *Microchannel*

The microchannel is fabricated by molding liquid polydimethylsiloxane (PDMS) onto a silicon master mould, baking it and peeling it off. The PDMS replica is then bonded onto a glass lamella by air plasma (Plasma cleaner, Harrick). The channel

Please cite this article as: Gires, P.-Y., et al., Transient behavior and relaxation of microcapsules with a cross-linked human serum albumin membrane. Journal of the Mechanical Behavior of Biomedical Materials (2015), http://dx.doi.org/10.1016/j.jmbbm.2015.09.008

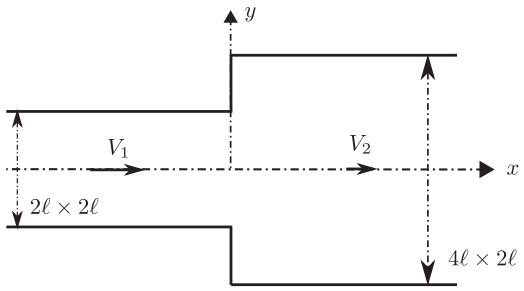

Fig. 1 – Geometry of the microsystem consisting of a square section ($2\ell \times 2\ell$) channel opening in a co-axial rectangular ($4\ell \times 2\ell$) channel.

consists of two co-axial parts: a square tube of side 2ℓ followed by a rectangular tube of cross-section $4\ell \times 2\ell$. As indicated in Fig. 1, x=0 corresponds to the location where the cross-section changes from square to rectangular. In practice, a typical microsystem used to conduct the experiments has a square channel of height $h = 105 \pm 1$ μm and width $w_1 = 107 \pm 1$ μm, and a rectangular channel of the same height $h = 105 \pm 1$ μm but width $w_2 = 206 \pm 1$ μm. The aspect ratio is thus $w_2/h = 1.96$ in the present case. The characteristic channel dimension ℓ can then be defined as $2\ell = \sqrt{w_1 \times h} = 106$ μm.

2.3. *Capsule flow observation*

A dilute suspension of capsules is prepared by re-suspending a volume of the stored HSA20 or HSA30 capsules in pure glycerol (e.g. 40 μL in 2 mL).

The suspension is dilute enough to ensure that the capsules will not interact with one another in the microchannel. The temperature of the experiment is monitored in order to get a precise value of the viscosity μ of the suspending fluid. Its viscosity is measured to be $\mu = 1.19$ Pa s at 20 °C (Couette viscometer Thermo Haake 1). The use of a very viscous bulk fluid is dictated by the substantial capsule deformation that has to be induced in order to characterize the membrane mechanical properties. The channel length is as short as possible ($\sim$1 cm) to minimize the large hydraulic resistance while ensuring that steady Poiseuille flow conditions are established over a long enough tube portion to make meaningful experiments (Lefebvre et al., 2008). The microsystem and tube connections have also been designed to resist 4–5 bars of internal pressure. No subsequent variation of the channel width could actually be measured: it is prevented by the thick lateral walls, the microchannel being imprinted in a PDMS patch about 2.5 cm in width and 4 cm in length. Even though it existed, the deviation of the square section channel from a pure square shape is assured to remain well below 5%: under this limit, Sévénié et al. (2015) have found no loss in accuracy of the inverse analysis technique.

A 1 mL glass syringe (Fortuna Optima) is filled with the suspension, taking care that no air bubble remains in either the syringe or the silicon connection tube to minimize throughput variations. The suspension is injected into the microfluidic system by means of a syringe pump (KDS100, KD Scientific) at different flow rates $Q = 0.05$–0.3 mL/h. The

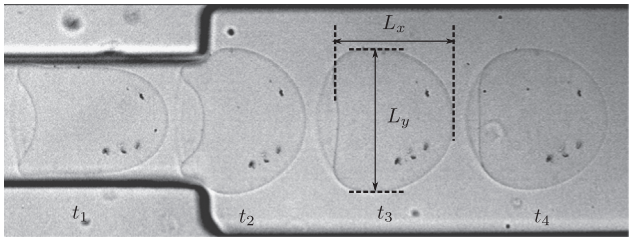

Fig. 2 – Successive profiles of a capsule: $t_2 - t_1 = 84$ ms, $t_3 - t_1 = 202$ ms, $t_4 - t_1 = 332$ ms.

experiments are run continuously over one hour or more depending on the set flow rate. Measurements of the capsule deformation and velocity are taken when the flow conditions in the microsystem are established. The mean velocity of the suspending fluid is considered as an unknown and determined by inverse analysis from the capsule deformation and velocity measured in the square channel.

The capsules are observed with a ×20 magnification transmission microscope (Leica DM IL LED), which is connected to a high resolution high-speed camera (FASTCAM SA3 Photron) through a ×1 C-mount (Leica). The microscope is focused on the channel center plane. The capsule profile is observed in the xy-plane. The images are recorded at 5000 frames per second, with an exposure time of 0.05 ms and an observation field of 256 × 768 pixels. The calibration scale is 0.425 μm/pixel. The observation field is far enough from the entrance (about 3 mm, i.e. 50ℓ) to consider that the capsule has reached a steady state in the square tube.

Fig. 2 shows successive experimental images of a HSA20 capsule. Because of the too low contrast of the image, it has not been possible to do an automatic extraction of the capsule deformed shapes: the profiles are extracted manually from the images by placing about hundred points at the center of the dark line of the capsule contour using ImageJ. In the square section, the geometrical quantities that are determined from the capsule shapes are the surface S of the profile, the maximum longitudinal length L_x and the axial length L_a (from which we can deduce the parachute depth $L_x - L_a$); the capsule velocity v_c is obtained from two successive images. In the rectangular section, we measure the maximum longitudinal length L_x and the transversal length L_y as functions of time (Fig. 2). All the lengths are measured with an accuracy of ± 1 pixel, which corresponds to ± 0.5 μm.

2.4. *Determination of the membrane elastic shear modulus*

For each capsule, an inverse analysis can be performed on its deformed profile in the square channel to yield the surface shear elastic modulus of the membrane. The method was developed by Hu et al. (2013) and is briefly presented here.

A full numerical model of the motion of an initially spherical capsule with radius a in a square section channel of side 2ℓ has been designed under Stokes flow conditions (Hu et al., 2012). The external and internal fluid viscosities are equal and denoted μ. The mean flow velocity in the channel is V_1. The capsule membrane is assumed to very thin and devoid of bending resistance. It is treated as a hyperelastic

Please cite this article as: Gires, P.-Y., et al., Transient behavior and relaxation of microcapsules with a cross-linked human serum albumin membrane. Journal of the Mechanical Behavior of Biomedical Materials (2015), http://dx.doi.org/10.1016/j.jmbbm.2015.09.008

surface with surface shear elastic modulus G_s (N/m). Different constitutive laws, strain-softening or strain-hardening, can be assumed for the membrane. Previous studies have investigated which law was the most adequate for albumin capsules, whether the membrane is made of ovalbumin (Chu et al., 2011) or human serum albumin (Hu et al., 2013). Strain-hardening laws, such as the Skalak et al. law (Skalak et al., 1973), have been shown in both cases to fail reproducing the measured capsule deformation. The latter is, however, well reproduced by the neo-Hookean law, which provides good results for the capsules whether they are subjected to small or moderate deformation. The study of de Loubens et al. (2015) indicates that compressibility effects in the membrane material may start playing a role, when the HSA capsules are subjected to large deformation. Since no such flow conditions are considered here (the elongational ratio is on average 1.04 with 1.07 as maximum value) and since all the constitutive laws reduce to the Hooke's law in the small deformation regime, the strain-softening neo-Hookean law was selected in the numerical model.

Apart from the membrane constitutive law, the main problem parameters are the confinement ratio a/ℓ and the relative flow strength as measured by the non-dimensional capillary number $Ca = \mu V/G_s$, which compares the viscous friction force of the capsule in the external flow to the membrane deformation force. In the square channel, the mean velocity V of the external flow is V_1.

The problem is solved by coupling a boundary integral method to compute the fluid flow and a finite element method to compute the membrane mechanics. The equations are solved in a reference frame moving with the capsule center of mass, so that the capsule remains centered in the tube domain. The advantage of the procedure is that only the boundaries of the flow domain (channel wall, entrance and exit sections, capsule surface) are discretized and meshed. At steady-state, the membrane and thus the internal fluid are motionless.

The model outputs are the capsule centroid velocity v_c and the steady deformed capsule shape as quantified by S, L_x and L_a. Since experimentally, all that can be observed is the projection of the deformed profile in the xy-plane, we define an apparent capsule radius $a_{app} = (2S\ell)^{1/3}$ and compute numerically the ratio a_{app}/ℓ. A database has been designed that relates S/ℓ^2, L_x/ℓ, L_a/ℓ, a_{app}/ℓ and v_c/V_1 to Ca and a/ℓ. The principle of the inverse analysis then consists of measuring the experimental values of L_x/ℓ, L_a/ℓ, S/ℓ^2 and searching the database for the values of a/ℓ and Ca for which we get the same numerical values of the geometrical parameters within some tolerance due to the experimental errors. From these values of a/ℓ and Ca, the database provides the corresponding velocity ratio v_c/V_1. The surface shear elastic modulus is then given by

$$G_s = \frac{\mu v_c}{Ca(v_c/V_1)} \tag{1}$$

where μ and v_c are measured experimentally. The capillary number is thereafter denoted Ca_1 in the square channel (and Ca_2 in the rectangular channel respectively). The procedure works best when the capsule and the channel have comparable cross dimensions to ensure a sufficient deformation of the particle (Hu et al., 2013). Note that another by-product of the inverse procedure is the estimation of the mean flow velocity V_1 in the square channel.

Table 1 – Determination of the membrane elastic modulus for HSA20 capsules flowing in the square channel.

a/ℓ	Ca_1	G_s (mN/m)	$\Delta G_s/G_s$ (%)	v_c (mm/s)	V_1 (mm/s)
1.10	0.054	33.14	15	1.79	1.52
1.11	0.050	44.01	16	2.13	1.80
1.11	0.055	34.44	12	1.88	1.58
1.11	0.056	40.37	15	2.20	1.87
1.14	0.047	53.81	17	2.42	2.12
1.15	0.050	28.78	14	1.35	1.16
1.16	0.042	57.80	17	2.36	2.08

Table 2 – Determination of the membrane elastic modulus for HSA30 capsules flowing in the square channel.

a/ℓ	Ca_1	G_s (mN/m)	$\Delta G_s/G_s$ (%)	v_c (mm/s)	V_1 (mm/s)
1.03	0.062	118.2	21	7.00	5.84
1.05	0.058	108.5	18	6.00	5.06
1.07	0.055	119.6	19	6.25	5.33
1.09	0.058	102.0	14	5.84	4.90
1.10	0.051	97.9	16	4.73	4.04
1.11	0.048	127.3	19	5.74	4.92
1.12	0.044	129.3	22	5.20	4.61
1.13	0.047	182.6	18	7.99	6.87
1.14	0.046	128.7	18	5.58	4.84

This procedure is applied to a population of 7 HSA20 and 9 HSA30 capsules in the size range $a/\ell \in [1.03, 1.17]$ with results shown in Tables 1 and 2. The maximum uncertainty on the value of G_s is around 20%, which is within the experimental uncertainties. Variations are most likely due to the fabrication process or to the transfer into glycerol. The next to last capsule of Table 2, however, has a high value of G_s, for which we have no explanation. We have still kept the capsule having no good reason to exclude it. The capsule membrane rigidity increases significantly with the HSA concentration. Indeed, for the same size, the HSA20 capsules have a mean surface shear elastic modulus $G_s = 42$ mN/m, while the corresponding modulus of the HSA30 capsules is roughly three times larger at $G_s = 124$ mN/m.

3. Analysis of the capsule relaxation

Typical relaxation curves giving the time evolution of the longitudinal L_x and transversal L_y lengths of the capsule are shown in Fig. 3. At time t=0, the nose of the capsule is at x=0 (i.e. at the junction between the square and rectangular sections). When the capsule enters the rectangular section, it is compressed in the axial direction because the flow is slower than in the square section: this phenomenon is apparent from the decrease of L_x. After a time of order ℓ/v_c, the capsule nose has advanced by ℓ into the rectangular section and the lateral expansion begins, as is apparent from the sudden increase of L_y. At time $t = t_e$, the rear of the

Please cite this article as: Gires, P.-Y., et al., Transient behavior and relaxation of microcapsules with a cross-linked human serum albumin membrane. Journal of the Mechanical Behavior of Biomedical Materials (2015), http://dx.doi.org/10.1016/j.jmbbm.2015.09.008

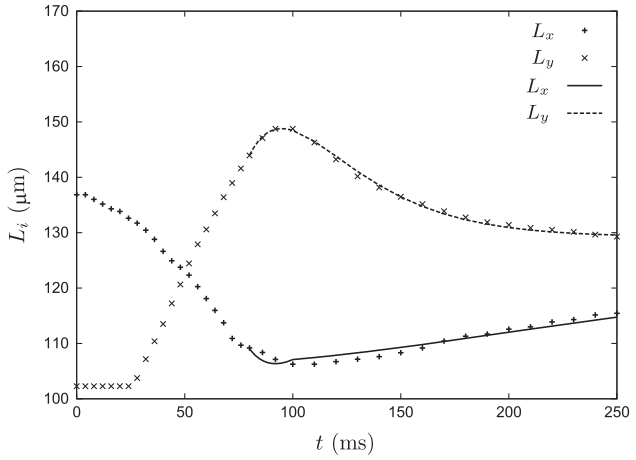

Fig. 3 – Time evolution of (L_x, L_y). The cross symbols represent the experimental data and the lines the fit with Eq. (2). The experimental data are fitted from time t_e onwards, when the rear of the capsule exits the square channel.

capsule exits from the square pore: the lateral expansion and overshoot of L_y are mostly due to the transient flow in the sudden expansion. The subsequent decrease of L_y and increase of L_x correspond to the adaptation to the steady flow conditions in the rectangular section.

We note that L_y reaches a stationary value much faster that L_x, which is not quite at equilibrium at the end of the visualization window. The reason for the slow time relaxation of L_x is linked to the behavior of the capsule rear, which has to adapt its curvature to the new flow conditions. This phenomenon takes time because the shear stress is very low in the middle of the channel: the capsule is thus mainly subjected to small pressure forces. Furthermore, the membrane tensions in the reverse curvature area are small, so that elastic shape recovery forces are small. This phenomenon is visible on the last picture of Fig. 2, where we can see that the rear parachute is still present. It is thus difficult to follow the full axial relaxation of the capsule experimentally, since this would mean increasing the observation field of the microscope, and thus decreasing the magnification to the detriment of precision.

For $t \geq t_e$, the time responses of L_x and L_y are fitted with a linear-exponential function classically used to model the current intensity response to a potential step in a critically damped RLC circuit:

$$L_i(t) = [L_i(0) - L_{i\infty} - \alpha_i(t - t_e)]e^{-(t-t_e)/\tau_i} + L_{i\infty}, \quad i = (x, y), \tag{2}$$

where $L_{i\infty}$ is the long-time asymptotic value of L_i. The parameters α_i, τ_i and $L_{i\infty}$ are determined using a least square fit between the experimental curve and the correlation equation (2). This correlation law allows us to capture the overshoot and the exponential decrease.

The results for HSA20 and HSA30 capsules are shown in Tables 3 and 4. For HSA20 capsules, the transversal response time τ_y (average value 24 $\pm$7 ms) is about half the axial response time τ_x (average value 50$\pm$10 ms). The same conclusion applies to HSA30 capsules, for which τ_y (average value 8$\pm$1 ms) is also half τ_x (average value 16$\pm$2 ms). This

Table 3 – Transient lateral response times for HSA20 capsules when they exit the square channel and enter the rectangular channel.

V_2 (mm/s)	τ_x (ms)	τ_y (ms)	$\tau_x V_2/\ell$	$\tau_y V_2/\ell$
0.81	56	26	0.84	0.39
0.96	50	21	0.89	0.38
0.84	48	28	0.75	0.43
1.00	43	21	0.80	0.39
1.13	45	20	0.94	0.42
0.62	70	37	0.82	0.43
1.11	38	18	0.78	0.37

Table 4 – Transient lateral response times for HSA30 capsules when they exit the square channel and enter the rectangular channel.

V_2 (mm/s)	τ_x (ms)	τ_y (ms)	$\tau_x V_2/\ell$	$\tau_y V_2/\ell$
3.11	15	9	0.87	0.50
2.70	18	9	0.89	0.43
2.84	18	9	0.92	0.49
2.61	19	10	0.93	0.47
2.15	17	6	0.67	0.25
2.62	17	9	0.80	0.45
2.45	14	8	0.62	0.38
3.66	12	6	0.84	0.43
2.58	15	9	0.74	0.42

corroborates the fact that the capsule takes a long time to adapt its axial length and that it is just as efficient from the experimental point of view to monitor only the transversal response.

To account for differences in local flow conditions from one capsule to the other and eliminate this effect, we normalize the response time with the flow conditions and compute $\overline{\tau_y} = \tau_y V_2/\ell$, where $V_2 \simeq V_1/2$ is the mean flow velocity in the rectangular channel. As shown in Tables 3 and 4, the non-dimensional response times $\overline{\tau_y}$ are almost equal and fall onto the same mean values, $\overline{\tau_y} = 0.40 \pm 0.02$ and $\overline{\tau_y} = 0.43 \pm 0.08$ for HSA20 and HSA30 capsules, respectively. The same conclusion applies to the corresponding mean values of the non-dimensional axial time, which are found to be $\overline{\tau_x} = 0.83 \pm 0.07$ and $\overline{\tau_x} = 0.81 \pm 0.11$ for HSA20 and HSA30 capsules, respectively.

4. Numerical model of relaxation in a rectangular channel

The numerical model of Hu et al. (2012), initially designed for a square section channel, is adapted to a rectangular channel with aspect ratio $w_2/h = 2$. Once the geometry of the channel has been defined, the only problem parameters are the confinement ratio a/ℓ and capillary number Ca_2. We further assume that the internal and external fluid viscosity is equal and that the membrane follows the neo-Hookean law.

The surface of the capsule is discretized with 1280 triangular curved P_2 elements and 2562 nodes, which correspond to a characteristic mesh size $\Delta h_C = O(0.1a)$. We first generate the

Please cite this article as: Gires, P.-Y., et al., Transient behavior and relaxation of microcapsules with a cross-linked human serum albumin membrane. Journal of the Mechanical Behavior of Biomedical Materials (2015), http://dx.doi.org/10.1016/j.jmbbm.2015.09.008

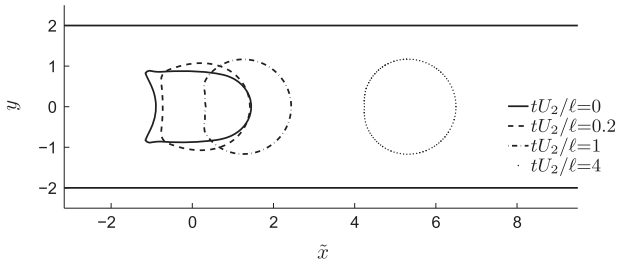

Fig. 4 – Successive profiles of a capsule suddenly immersed into a rectangular channel ($a/\ell = 1.1$, $Ca_2 = 0.025$). The $\tilde{x}$-axis is defined so that the capsule centroid is initially located at $\tilde{x} = 0$.

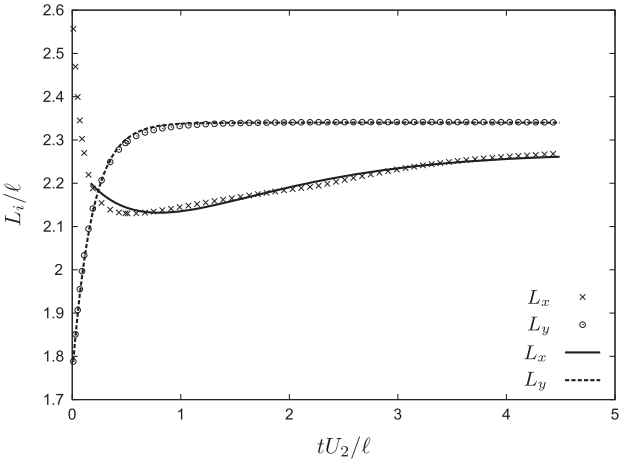

Fig. 5 – Time evolution of the transverse and axial lengths for $a/\ell = 1.1$ and $Ca_2 = 0.025$. The cross (L_x) and circle (L_y) symbols represent the values found numerically in the elastic case, and the full and dotted lines the corresponding correlations obtained using Eq. (2).

two-dimensional geometry of the tube cross-section and mesh it with unstructured triangular elements having a mesh size $\Delta h_S = O(0.14\ell)$. The corners of the rectangular cross-section have been rounded with an arccircle (radius Δh_S) in order to avoid corner effects when solving for the flow. The central section of the tube (of length 4ℓ) has a more refined mesh ($\Delta h_W = O(0.14\ell)$) than the inlet and outlet tube sections ($\Delta h_W = O(0.22\ell)$), each of length 6ℓ. Altogether, the mesh comprises 1905 nodes and 3768 elements for the rectangular tube.

We first use the model to compute the steady deformed profile that the capsule takes in the square channel of cross-section $2\ell \times 2\ell$ for various values of a/ℓ and Ca_1. At time $t=0$, we release the deformed profiles at the center of the rectangular channel $4\ell \times 2\ell$, and subject them to flow conditions corresponding to a capillary number $Ca_2 = Ca_1/2$ with the same confinement ratio a/ℓ. We then follow the time evolution of the capsule profiles as they adapt to the new flow conditions. Typical successive relaxation profiles are shown in Fig. 4. The corresponding time evolutions of the non-dimensional transversal L_y/ℓ and axial L_x/ℓ lengths are shown in Fig. 5, together with the fits corresponding to Eq. (2).

For $Ca_1 = 0.05$ and thus $Ca_2 = 0.025$, which correspond to the prevailing experimental conditions (Tables 1 and 2), we find that the transversal response time $\bar{\tau}_{ynum}$ increases slightly with a/ℓ. The axial time response is difficult to obtain as the correlation equation (2) cannot capture both the steep decrease of L_x/ℓ and the slow exponential recovery. The latter is due to the change of curvature at the rear of the capsule and if this phenomenon is difficult to capture experimentally, the same is true also for the numerical simulation. Altogether, the axial response time is about four times the transversal one (Table 5).

Table 5 – Numerical response times in a rectangular channel for $Ca_2 = 0.025$.

a/ℓ	1.0	1.1	1.2
$\bar{\tau}_{xnum}$	0.82	0.83	0.76
$\bar{\tau}_{ynum}$	0.17	0.18	0.22

5. Discussion and conclusion

We have studied the transient response of initially spherical capsules having a cross-linked human serum albumin membrane, as they flow through a sudden expansion. The microsystem consists of a square-section tube, long enough for capsules to reach a steady deformed shape, followed by a rectangular tube, in which the capsules relax progressively. The advantage of this channel configuration is to allow the characterization of both the membrane elastic properties in the square tube and of the capsule viscoelastic behavior in the rectangular tube.

5.1. *Surface shear elastic modulus of the capsule membrane*

We consider two capsule populations with a similar mean diameter of 119 μm, fabricated with either 20% or 30% human serum albumin solutions. Due to their amphiphilic properties, HSA proteins tend to adsorb at interfaces. As a consequence the surface concentration of HSA molecules is larger for the HSA30 than for the HSA20 capsules. It follows that the HSA30 capsules are more cross-linked than the HSA20 ones. This is corroborated by the fact that the capsule membrane rigidity is found to increase with the HSA concentration: the mean surface shear elastic modulus G_s is about three times larger for the HSA30 than for the HSA20 capsules.

5.2. *Capsule relaxation*

To characterize the relaxation of the capsules, we have followed the time-evolution of the deformed profiles and determined the corresponding intrinsic response times. We have shown that the transversal relaxation time τ_y is about half the axial response time τ_x: the capsule needs a longer time to change its axial length, as it involves a change of curvature at the rear. Experimentally, it is much easier to measure the transversal response time τ_y than the longer axial one τ_x. Since the two times provide equivalent results, it may be sufficient to only analyze the transversal relaxation to evaluate the capsule membrane properties.

Please cite this article as: Gires, P.-Y., et al., Transient behavior and relaxation of microcapsules with a cross-linked human serum albumin membrane. Journal of the Mechanical Behavior of Biomedical Materials (2015), http://dx.doi.org/10.1016/j.jmbbm.2015.09.008

Dimensional analysis shows that the intrinsic response time of a capsule scales as $\tau_c \sim \mu a/G_s$. We observe in Tables 1 and 2, that the transverse characteristic time τ_y is about three times longer for HSA20 (24± 7 ms) than for HSA30 capsules (8± 1 ms). This is due to the larger elastic modulus of the HSA30 capsules, which is about three times larger than the one of HSA20 capsules.

In order to have a measurable deformation of the HSA30 capsules, we had to use a flow rate, which was roughly three times the one used for HSA20 capsules (see Tables 1 and 2). The flow convective time $\tau_f = \ell/V_2$ is thus three times smaller for HSA30 than for HSA20 capsules: $\tau_f(HSA20) = 3\tau_f(HSA30)$. This explains why the response time scaled with the flow convective time $\overline{\tau}_y = \tau_y/\tau_f$ takes the same value for the two sets of experiments.

The capillary number, which was introduced as the ratio between viscous and elastic forces, may also be interpreted as the ratio between τ_c and the characteristic convection time τ_f, modulated by the confinement ratio:

$$Ca \sim \frac{\tau_c}{\tau_f}\frac{\ell}{a}. \tag{3}$$

The capillary number thus has the same value in the two sets of experiments.

5.3. *Influence of confinement*

Barthès-Biesel and Rallison (1981) have studied the relaxation of a capsule in an unbounded flow domain after cessation of a shear flow. In this case, the flow characteristic time is $\tau_f = 1/\dot{\gamma}$, where $\dot{\gamma}$ is the shear rate and the capillary number is $Ca_{sf} = \mu\dot{\gamma}a/G_s$. An analytical solution, valid for small capsule deformation (i.e. up to $Ca_{sf} \sim 0.07$, Lac et al., 2004), predicts that the non-dimensional relaxation time depends only on the initial capillary number:

$$\tau\dot{\gamma} = \frac{3(19\lambda+16)(2\lambda+3)}{5(19\lambda+24)\pm\sqrt{5377\lambda^2+14256\lambda+9792}}\frac{Ca_{sf}}{3}, \tag{4}$$

where λ is the ratio between the internal and external fluid viscosity. For $\lambda = 1$, we find $\tau\dot{\gamma} = 4.03Ca_{sf}$.

In our case, taking as characteristic time scale τ_f the convection time scale ℓ/V_2 instead of $1/\dot{\gamma}$, we find that the response time predicted by the unbounded flow theory (Eq. (4)) would be

$$\tau V_2/\ell = 4.03Ca_2 a/\ell. \tag{5}$$

Since $Ca_2 = 0.025$ and $a/\ell = 1.1$, we obtain $\tau V_2/\ell = 0.11$, which is of the same order of magnitude as the value simulated for a capsule with a purely elastic membrane flowing within a confined environment ($\overline{\tau_y} = 0.18$). Thus confinement does not seem to have a significant effect on the capsule response time.

5.4. *Viscoelasticity of the capsule membrane*

The experimental response time is compared with numerical results obtained for a capsule with a purely elastic membrane. The same flow situations prevail in the experimental and numerical cases, except for the initial conditions. Numerically, we have indeed neglected the effects of the exit from the square channel and of the flow in the sharp expansion in the numerical model, which has the advantage of significantly simplifying it. By essence, there is thus no transverse flow in the numerical simulation outside the one generated by the elastic recoil of the capsule as it deforms under flow. In the experiment, there is, however, a strong transverse flow directly downstream of the channel expansion. It is a consequence of the channel geometry and of the temporary partial blockage of the exit by the deformable capsule. This results in a sharp overshoot of the experimental value of L_y, which is not observed numerically; the differences between the numerical and experimental transient behaviors are less pronounced for L_x, as the transverse flow has a secondary effect on the axial velocity.

We find that the predicted numerical values of non-dimensional transverse response time $\overline{\tau}_y$ are about half the measured experimental ones for the two capsule populations (Table 5). As the difference is significant, it is likely due to some viscous effects in the membrane. The membrane viscoelasticity may come from some loose cross-linked HSA networks that can rearrange themselves during the flow transient phase.

In order to go further in the analysis of the experimental results and deduce an estimate of the membrane viscosity of the capsules, a full numerical model of a flowing viscoelastic capsule is necessary. Simulating the motion and deformation of deformable microcapsules under flow accounting for membrane viscoelasticity is challenging numerically. Only few studies have at present included membrane viscosity. Barthès-Biesel and Sgaier (1985) developed a small-deformation theoretical model of a capsule under simple shear flow, in which the membrane was assumed to follow the Kelvin–Voigt model. To our knowledge, only two numerical analyses have simulated the large deformation of capsules with a viscoelastic (Kelvin–Voigt) membrane with membrane viscosity μ_s. The first is by Diaz et al. (2001), who considered an initially spherical capsule subjected to a pure straining motion. In this case, the steady deformation does not depend on membrane viscosity as the membrane is motionless at steady state. They studied in detail the influence of membrane viscosity on the transient behavior towards steady state. The other study is by Yazdani and Bagchi (2013), who studied the motion of a capsule (initially spherical or ellipsoidal) in simple shear flow. They were mostly interested in the effect of membrane viscosity on the steady deformation and did not make a detailed study of its influence on the response time.

In our study, the capsule flows within a tube under high confinement: membrane viscosity has no effect on its stationary shape, and only influences the transient behavior. No numerical study has ever modeled the relaxation of a viscoelastic capsule after a change in flow regime within a confined tube.

The nearest study that can be used to estimate the order of magnitude of the membrane viscosity is the one by Diaz et al. (2001), in which they provided correlations of the response time as a function of the membrane and fluid viscosities

$$\dot{\gamma}\tau_{ve} = \dot{\gamma}\tau_e + A\eta, \tag{6}$$

where τ_{ve} and τ_e are the response times in the case of a viscoelastic and purely elastic capsule membrane,

Please cite this article as: Gires, P.-Y., et al., Transient behavior and relaxation of microcapsules with a cross-linked human serum albumin membrane. Journal of the Mechanical Behavior of Biomedical Materials (2015), http://dx.doi.org/10.1016/j.jmbbm.2015.09.008

respectively, $\dot{\gamma}$ the elongational flow shear rate, A a coefficient of the correlation law and $\eta = \mu_s/\mu a$ the surface-to-bulk viscosity ratio. We assume that the effect of the membrane viscosity on the response time is approximately the same for unconfined and confined flows. Thus taking $\dot{\gamma}\tau_{ve} = \overline{\tau}_y$, $\dot{\gamma}\tau_e = \overline{\tau}_{ynum}$ and A=0.0186 for the experimental capillary number of 0.025 (linear interpolation of the coefficient values, Diaz et al., 2001), we find $\eta \sim 12$, which indicates that the membrane viscosity cannot be neglected in the present experiment. We can then estimate the value of the capsule membrane viscosity: $\mu_s \sim 8 \times 10^{-4}$ N s/m. We find that the membrane viscosity of the HSA capsules is 3 orders of magnitude larger than the one of red blood cells (Chien et al., 1978) and about 30 times smaller than that of the nylon capsules studied by Chang and Olbricht (1993). All these values of membrane viscosities cannot be compared among one another, as they result from the composition of the membranes, which are completely different in each case.

Of course, one must keep in mind that this is only a rough estimate of the membrane viscosity order of magnitude, as channel flow and elongational flow configurations are different. These results will need to be confirmed by future numerical simulations of the relaxation of capsules flowing through microchannels with a sudden expansion.

Acknowledgments

The authors would like to thank Florence Edwards-Lévy (ICMR, Université de Reims Champagne Ardennes, France) for providing the microcapsules, the LAAS-CNRS (member of the RENATECH network) for the fabrication of the microsystem, and Van Tuan Dang for conducting the measurements.

The research study was funded by the French National Agency for Research (CAPSHYDR grant ANR-11-BS09-013 and Labex MS2T ANR-11-IDEX-0004-02 within the program "Investment for the Future") and by the French Ministry of Research (Pilcam2 grant). The sponsors played no role in the design of the study, collection, analysis and interpretation of data, writing of the manuscript or decision to submit the article for publication.

REFERENCES

Barthès-Biesel, D., 1991. Role of interfacial properties on the motion and deformation of capsules in shear flow. Physica A 172, 103–124.

Barthès-Biesel, D., Rallison, J.M., 1981. The time-dependent deformation of a capsule freely suspended in a linear shear flow. J. Fluid Mech. 113, 251–267.

Barthès-Biesel, D., Sgaier, H., 1985. Role of membrane viscosity in the orientation and deformation of a spherical capsule suspended in shear flow. J. Fluid Mech. 160, 119–135.

Chang, K.S., Olbricht, W.L., 1993. Experimental studies of the deformation and breakup of a synthetic capsule in extensional flow. J. Fluid Mech. 250, 587–608.

Chang, K.S., Olbricht, W., 1993. Experimental studies of the deformation and breakup of a synthetic capsule in steady and unsteady simple shear flow. J. Fluid Mech. 250, 609–633.

Chien, S., Sung, K., Skalak, R., Usami, S., Tözeren, A., 1978. Theoretical and experimental studies on viscoelastic properties of erythrocyte membrane. Biophys. J. 24, 463–487.

Chu, T., Salsac, A.-V., Leclerc, E., Barthès-Biesel, D., Wurtz, H., Edwards-Lévy, F., 2011. Comparison between measurements of elasticity and free amino group content of ovalbumin microcapsule membranes: discrimination of the cross-linking degree. J. Colloid Interf. Sci. 355 (1), 81–88.

de Loubens, C., Deschamps, J., Boedec, G., Leonetti, M., 2015. Stretching of capsules in an elongation flow, a route to constitutive law. J. Fluid. Mech. 767, R3.

de Loubens, C., Deschamps, J., Georgelin, M., Charrier, A., Edward-Lévy, F., Leonetti, M., 2014. Mechanical characterization of cross-linked serum albumin microcapsules. Soft Matter 10, 4561–4568.

Diaz, A., Barthès-Biesel, D., Pelekasis, N., 2001. Effect of membrane viscosity on the dynamic response of an axisymmetric capsule. Phys. Fluids 13 (12), 3835–3838.

Edwards-Lévy, F., 2011. Microparticulate drug delivery systems based on serum albumin. In: Serum Albumin: Structure, Functions and Health Impact. Nova Science Publishers, New York.

Hochmuth, R., Worthy, P., Evans, E., 1979. Red cell extensional recovery and the determination of membrane viscosity. Biophys. J. 26, 101–114.

Hu, X.-Q., Salsac, A.-V., Barthès-Biesel, D., 2012. Flow of a spherical capsule in a pore with circular or square cross-section. J. Fluid Mech. 705, 176–194.

Hu, X.-Q., Sévénié, B., Salsac, A.-V., Leclerc, E., Barthès-Biesel, D., 2013. Characterizing the membrane properties of capsules flowing in a square-section microfluidic channel: effects of the membrane constitutive law. Phys. Rev. E 87 (6), 063008.

Koleva, I., Rehage, H., 2012. Deformation and orientation dynamics of polysiloxane microcapsules in linear shear flow. Soft Matter 8, 3681–3693.

Kühtreiber, W.M., Lanza, R.P., Chick, W.L. (Eds.), 1999. Cell Encapsulation Technology and Therapeutics. Springer Science & Business Media, New York.

Lac, E., Barthès-Biesel, D., Pelakasis, A., Tsamopoulos, J., 2004. Spherical capsules in three-dimensional unbounded stokes flows: effect of the membrane constitutive law and onset of buckling. J. Fluid Mech. 516, 303–334.

Lam, P.L., Gambari, R., 2014. Advanced progress of microencapsulation technologies: in vivo and in vitro models for studying oral and transdermal drug deliveries. J. Control. Release 178, 25–45.

Leclerc, E., Kinoshita, H., Fujii, T., Barthès-Biesel, D., 2012. Transient flow of microcapsules through convergent–divergent microchannels. Microfluid. Nanofluid. 12, 761–770.

Lefebvre, Y., Leclerc, E., Barthès-Biesel, D., Walter, J., Edwards-Lévy, F., 2008. Flow of artificial microcapsules in microfluidic channels: a method for determining the elastic properties of the membrane. Phys. Fluids 20 123102(10).

Orive, G., Hernández, R.M., Gascón, A.R., Calafiore, R., Chang, T.M. S., de Vos, P., Hortelano, G., Hunkeler, D., Lacík, I., Pedraz, J.L., 2004. History, challenges and perspectives of cell microencapsulation. Trends Biotechnol. 22, 87–92.

Rehage, H., Husmann, M., Walter, A., 2002. From two-dimensional model networks to microcapsules. Rheol. Acta 41, 292.

Risso, F., Collé-Paillot, F., Zagzoule, M., 2006. Experimental investigation of a bioartificial capsule flowing in a narrow tube. J. Fluid Mech. 547, 149–173.

Sévénié, B., Salsac, A.-V., Barthès-Biesel, D., 2015. Characterization of capsule membrane properties using a microfluidic photolithographied channel: consequences of tube non-squareness. Proc. IUTAM 16, 106–114.

Skalak, R., Tozeren, A., Zarda, R.P., Chien, S., 1973. Strain energy function of red blood cell membranes. Biophys. J. 13, 245–264.

Please cite this article as: Gires, P.-Y., et al., Transient behavior and relaxation of microcapsules with a cross-linked human serum albumin membrane. Journal of the Mechanical Behavior of Biomedical Materials (2015), http://dx.doi.org/10.1016/j.jmbbm.2015.09.008

Tomaiuolo, G., Barra, M., Preziosi, V., Cassinese, A., Rotolid, B., Guido, S., 2011. Microfluidics analysis of red blood cell membrane viscoelasticity. Lab Chip 11, 449–454.

Tran-Son-Tay, R., Sutera, S., Rao, P., 1984. Determination of red blood cell membrane viscosity from rheoscopic observations of tank-treading motion. Biophys. J. 46, 65–72.

Walter, A., Rehage, H., Leonhard, H., 2000. Shear-induced deformation of polyamid microcapsules. Colloid Polym. Sci. 278, 169–175.

Yazdani, A., Bagchi, P., 2013. Influence of membrane viscosity on capsule dynamics in shear flow. J. Fluid Mech. 718, 569–595.

Please cite this article as: Gires, P.-Y., et al., Transient behavior and relaxation of microcapsules with a cross-linked human serum albumin membrane. Journal of the Mechanical Behavior of Biomedical Materials (2015), http://dx.doi.org/10.1016/j.jmbbm.2015.09.008